Title

TBX3 Directs Cell-Fate Decision toward Mesendoderm

Journal

Stem Cell Reports, 1(3)

ISSN

2213-6711

Authors

Weidgang, Clair E
Russell, Ronan
Tata, Purushothama R
et al.

Publication Date

2013-09-01

DOI

10.1016/j.stemcr.2013.08.002

Stem Cell Reports
Article
OPEN ACCESS

TBX3 Directs Cell-Fate Decision toward Mesendoderm

Clair E. Weidgang,[1,2,13] Ronan Russell,[1,3,13] Purushothama R. Tata,[2,4,13,15] Susanne J. Kühl,[4] Anett Illing,[1] Martin Müller,[1] Qiong Lin,[7] Cornelia Brunner,[5] Tobias M. Boeckers,[6] Kerstin Bauer,[8] Apriliana E.R. Kartikasari,[9] Yanchun Guo,[2,4] Melanie Radenz,[2,4] Christof Bernemann,[10] Matthias Weiß,[11] Thomas Seufferlein,[1] Martin Zenke,[7] Michelina Iacovino,[12,16] Michael Kyba,[12] Hans R. Schöler,[10] Michael Kühl,[4] Stefan Liebau,[6,14,*] and Alexander Kleger[1,14,*]

[1]Department of Internal Medicine I
[2]International Graduate School in Molecular Medicine
[3]Graduate College 1041
[4]Institute for Biochemistry and Molecular Biology
[5]Institute for Physiological Chemistry
[6]Institute for Anatomy & Cell Biology
Ulm University, 89081 Ulm, Germany
[7]Department of Cell Biology, Institute for Biomedical Engineering, Medical Faculty, RWTH Aachen University, 52074 Aachen, Germany
[8]Institute of Molecular Medicine and Max-Planck-Research Group on Stem Cell Aging, 89081 Ulm, Germany
[9]Department of Medicine, University of California, Los Angeles, CA 90095, USA
[10]Department of Cell and Developmental Biology, Max Planck Institute for Molecular Biomedicine, 48149 Münster, Germany
[11]University Medical Centre, Renal Department, Centre for Clinical Research, 79106 Freiburg, Germany
[12]Department of Pediatrics, Lillehei Endowed Scholar, Lillehei Heart Institute, University of Minnesota, Minneapolis, MN 55455, USA
[13]These authors contributed equally to this work
[14]These authors contributed equally to this work
[15]Present address: Center for Regenerative Medicine, Harvard Stem Cell Institute, Massachusetts General Hospital, Boston, MA 02114, USA
[16]Present address: Department of Pediatrics, Division Medical Genetics, Harbor University of California, Los Angeles, LABioMED, USA
*Correspondence: stefan.liebau@uni-ulm.de (S.L.), alexander.kleger@uni-ulm.de (A.K.)
http://dx.doi.org/10.1016/j.stemcr.2013.08.002

SUMMARY

Cell-fate decisions and pluripotency are dependent on networks of key transcriptional regulators. Recent reports demonstrated additional functions of pluripotency-associated factors during early lineage commitment. The T-box transcription factor TBX3 has been implicated in regulating embryonic stem cell self-renewal and cardiogenesis. Here, we show that TBX3 is dynamically expressed during specification of the mesendoderm lineages in differentiating embryonic stem cells (ESCs) in vitro and in developing mouse and *Xenopus* embryos in vivo. Forced TBX3 expression in ESCs promotes mesendoderm specification by directly activating key lineage specification factors and indirectly by enhancing paracrine Nodal/Smad2 signaling. TBX3 loss-of-function analyses in the *Xenopus* underline its requirement for mesendoderm lineage commitment. Moreover, we uncovered a functional redundancy between TBX3 and Tbx2 during *Xenopus* gastrulation. Taken together, we define further facets of TBX3 actions and map TBX3 as an upstream regulator of the mesendoderm transcriptional program during gastrulation.

INTRODUCTION

Pluripotent embryonic stem cells (ESCs) or induced pluripotent stem cells (iPSCs) are characterized by continuous self-renewal while maintaining the potential to differentiate into cells of all three germ layers. The regulatory networks of maintaining ESC pluripotency have been described in great detail (Ying et al., 2008), and, similarly, there is a vast wealth of knowledge on key players that regulate differentiation of pluripotent stem cells. Multiple pathways including WNTs (wingless-related MMTV integration site), transforming growth factor (TGF)-β, BMP (bone morphogenetic protein), and fibroblast growth factor (FGF) signaling act in concert with a combination of key transcription factors to coordinate lineage commitment (Blair et al., 2011).

Recent reports suggest that pluripotency-associated transcription factors engage in additional functions during the early phases of germ layer specification and commitment. OCT4 and NANOG promote mesodermal as well as endodermal fate and limit neuroectoderm differentiation. In contrast, SOX2 enhances neuroectoderm while restricting mesoderm and endoderm development. Accordingly, groups of pluripotency factors were defined as mesendoderm class (e.g., OCT4, Nanog, KLF5) or neuroectoderm class (e.g., SOX2, RBPJ) ESC genes (Thomson et al., 2011).

Preceding mouse gastrulation, the rather symmetrical embryo is prepatterned by regional differences in gene expression and fluctuating levels of signaling pathways along the embryonic axes. Signaling gradients including NODAL and canonical WNT at the posterior pole of the embryo promote the formation of the primitive streak, accompanied by the expression of early differentiation marker genes (Arnold and Robertson, 2009).

As one of the early events during gastrulation, definitive endoderm (DE) and anterior mesoderm derivatives, including cardiovascular and head mesenchyme progenitors, are generated from a transient precursor cell population located in the region of the anterior primitive streak. This cell population is commonly referred to as mesendoderm and is marked by the expression of genes including Chordin (*Chrd*), Eomesodermin (*Eomes*), Foxa2, Goosecoid (*Gsc*), and LIM-homeobox1 (*Lhx1*) (Tada et al., 2005).

An evolutionarily conserved regulatory network, including NODAL and BMP signaling, controls mesendoderm induction as well as successive specification of DE and mesoderm lineages (Zorn and Wells, 2009). Members of the T-box transcription factor family exert highly specific and crucial functions throughout development (Arnold and Robertson, 2009). During gastrulation EOMES regulates the specification of DE and cardiovascular mesoderm from the anterior primitive streak region, Brachyury (*T*) is required for expansion of the posterior mesoderm and TBX6 specifies intermediate primitive streak derivatives (Pereira et al., 2011). In midgestation murine embryos, TBX3 plays important roles in cardiac chamber specification, hepatic bud expansion, and limb patterning (Chapman et al., 1996; Hoogaars et al., 2007). Heterozygous mutations in the human *Tbx3* gene were identified in the Ulnar-mammary syndrome, characterized by limb, genital, apocrine, and cardiac abnormalities (Bamshad et al., 1997). In pluripotent stem cells, TBX3 helps to maintain pluripotency by mediating LIF/STAT signaling (Niwa et al., 2009) and facilitates reprogramming by direct binding and activation of the OCT4 promoter (Han et al., 2010). TBX3 modulates the formation of extraembryonic, visceral endoderm (VE) by directly activating GATA6 expression (Lu et al., 2011) and acts as a downstream activator of WNT signaling (Price et al., 2012). In contrast, TBX3 is one of the transcriptional regulators that is highly enriched in DE progenitor cells (Cheng et al., 2012). Further, TBX3 in concert with the histone demethylase JMJD3 and EOMES are involved in endoderm formation (Kartikasari et al., 2013).

Here, we identified a function for TBX3 in early lineage commitment toward DE and anterior mesoderm derivatives. In murine and *Xenopus* embryos, TBX3 expression coincides with gastrulation onset, and TBX3 loss of function in *Xenopus* affects mesendoderm marker gene expression and impairs gastrulation. Our data suggest that TBX3 promotes lineage commitment toward DE and anterior mesoderm derivatives in a dual fashion: first, TBX3 directly regulates key lineage determining transcription factors (cell autonomous). Second, we demonstrate a central role for TBX3 in Nodal-mediated paracrine signaling (non-cell autonomous).

RESULTS

TBX3 Expression Is Dynamically Regulated in Early Embryonic Development

Published transcriptome data of preimplantation stage mouse embryos (Guo et al., 2010) indicated moderate *Tbx3* expression beginning at the 4-cell stage, increasing toward the blastocyst stage (Figure 1A). To determine early embryonic expression of TBX3, we analyzed messenger RNA (mRNA) and protein distribution of TBX3 in pre- and postimplantation stage embryos. Immunofluorescence (IF) analysis demonstrated TBX3 colocalizing with OCT4 in the ICM of E3.5 blastocysts, whereas protein was absent at the 2-cell stage (Figure 1B; data not shown). mRNA in situ hybridization (ISH) on early pregastrulation stage embryos (E6.25) showed *Tbx3* expression in the proximal posterior pole of the epiblast in addition to the reported expression in the extraembryonic structures (Figure 1C, left panel). At midgastrulation stage (E7.5) *Tbx3* expression was predominantly found in the extraembryonic VE and in a ring of mesoderm close to the embryonic-extraembryonic intersection (Figure 1C, right panel). At late gastrulation stages (E7.75, E8.25), *Tbx3* RNA was observed in the cardiac crescent and the tail region of the embryo (Figure 1D). We found TBX3-reporter expression in E6.5 embryos (GFP expression driven by a 160 kbp bacterial artificial chromosome with TBX3 and flanking sequences [Horsthuis et al., 2009]) in extraembryonic structures as well as in the proximal posterior epiblast (Figure 1E). We then wondered whether TBX3 expression is conserved in different species and performed semi quantitative RT-PCR and ISH for *tbx3* mRNA on different stages of *Xenopus* embryos. We detected a weak maternal *tbx3* expression with a marked increase at the onset of gastrulation (stage 10, Figure 1F). At later gastrulation stages, *tbx3* mRNA was readily detectable in early mesodermal cells and in the developing heart region (Figure 1G).

In summary, our results demonstrate that TBX3 is dynamically regulated during early development and expressed at specific sites of gastrulation onset in both mouse and *Xenopus* embryos.

TBX3 Promotes ESC Differentiation toward Mesoderm and Endoderm

During embryoid body (EB) differentiation, we observed moderate *Tbx3* mRNA expression in undifferentiated ESCs (Figure 2A) followed by a downregulation during early differentiation (days 1 and 2). Subsequently, expression rapidly increased with a peak on day 3, falling again until day 6. Comparable results were achieved by western blot (WB) and IF (Figures 2B and 2C). Published transcriptome data of several differentiating ESC lines

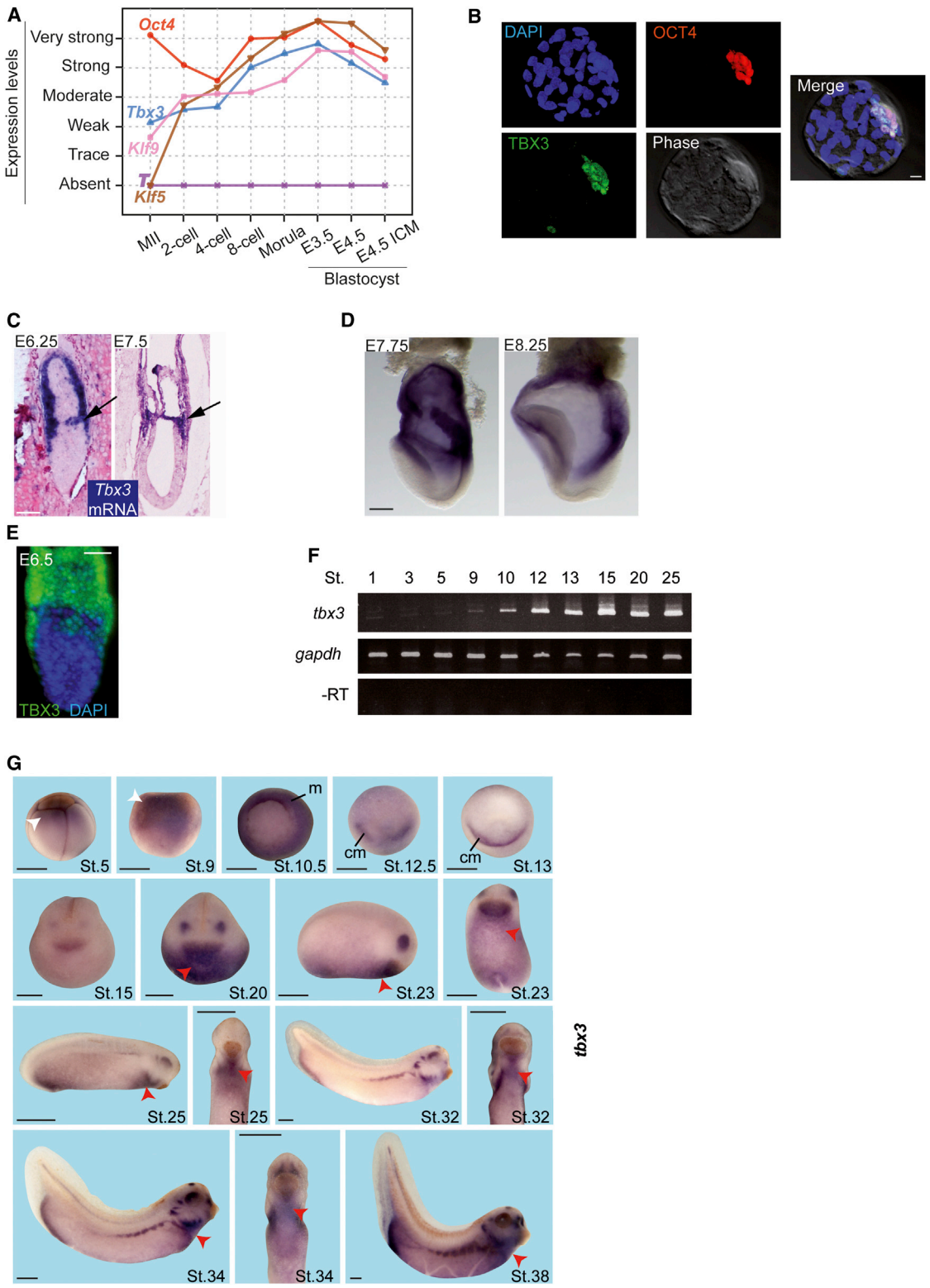

Figure 1. TBX3 Expression in Developing Mouse and *Xenopus* Embryos

(A) *Tbx3* (blue) in preimplantation embryos plotted with other mesendoderm class ESC genes (*Oct4*, red; *Klf5*, brown; *Klf9*, pink; *T*, violet). Data were obtained upon reanalysis of published data sets.

(legend continued on next page)

confirm these findings (http://www.fungenes.org). Interestingly, elevated TBX3 levels coincided with the expression of critical lineage determining factors such as EOMES, T, SOX17, and MESP1 in qPCR and IF (Figures 2D–2G). TBX3 expression was found to colocalize with the early differentiation markers EOMES (67% ± 7%), T (46% ± 2%), and SOX17 (51% ± 8%) at day 4 of EB differentiation (Figure 2H). To test whether TBX3 is specifically enhanced in subsets of differentiating ESCs, we used reporter cell lines to trace transcription of *T* and *Sox17*, markers of mesoderm and endoderm. After differentiation for 4 days, T- or SOX17- positive cells were fluorescence-activated cell sorting (FACS)-purified, and remaining pluripotent cells were excluded from the analyses using the pluripotency reporter DPPA4-RFP or SSEA1 staining (Figures 2I and 2K; data not shown). qPCR shows enriched *Tbx3* expression in cells committed toward the mesoderm or endoderm cell fate (Figures 2J and 2L) and IF confirmed that SOX17 or T positive-sorted cells coexpress TBX3 (Figures 2M and 2N). These results indicate that endogenous TBX3 expression in differentiating ESCs is correlated with mesendoderm cell-fate specification.

A study reported that TBX3 improved iPSC reprogramming and used chromatin immunoprecipitation (ChIP) sequencing to identify genes directly regulated by TBX3 during pluripotent conditions (Han et al., 2010). Reanalyzing these data, we found that TBX3 binding was enriched on the promoters of promoting pluripotency factors including *Klf5*, *Klf4*, and *Oct4* and promoters of key lineage determining factors such as *Sox9*, *Nkx6.1*, and *Eomes* (Figure S1 available online). This suggests that TBX3 may play an important role during the switch from pluripotency to differentiation toward the mesendodermal lineage.

In order to test this hypothesis, we generated a targeted, inducible TBX3 expression allele in ESCs to allow for the temporally regulated and dose-dependent expression of TBX3 (iTBX3 ESCs; Figures S2A–S2D). We used a recombination system in the HPRT locus, where a doxycycline (Dox)-inducible promoter regulates expression of the *Tbx3* mRNA (Iacovino et al., 2011). This *Tbx3* allele was homogenously induced in all cells upon Dox-exposure. Using EB differentiation, we assessed the effects of TBX3 overexpression on marker genes of all three germ layers (Figure 3A). In TBX3-overexpressing cells, enhanced differentiation toward mesoderm and endoderm progenitors was confirmed by IF for EOMES, T, and SOX17 (IF and WB) in day 4 EBs (Figure 3B; Figures S2E–S2I) and early marker transcripts of mesendoderm (*Chrd*, *Gsc*, *Eomes*, *Lhx1* [Lim1] (Figure 3C); *FoxA1*, *Lefty1*, *Cer1* (Figure S2J; data not shown), mesoderm (*T*, *Mesp1*, *Nkx2.5*; Figure 3D), and endoderm (*FoxA2*, *Sox17*, *Hex1*; Figure 3D) were upregulated. Marker genes specific for the pregastrula epiblast (*Fgf5*, *Otx2*, and *Nanog*) were also significantly upregulated after TBX3 induction (Figure S2K). In contrast, ectoderm (*Pax6*, *Fgf4*, *Noggin*, *Gbx2*) and trophectoderm-specific genes (*Cdx2*, *Hand1*, *Wnt6*, *Fgfr2*) were reduced (Figures 3E, S2L, and S2M). Small-hairpin-RNA (shRNA)-mediated knockdown of TBX3 diminished *Eomes* and *T* transcription (Figure 3F). In line with previous reports (Lu et al., 2011), marker genes of primitive endoderm, such as *Hnf4α*, *Hnf1β*, *Gata6*, and *AFP*, were increased following TBX3 overexpression (Figure S2N).

To generate a global view of TBX3-induced ESC differentiation, we performed genome-wide transcriptional profiling followed by gene set enrichment analysis. Groups of differentially regulated genes were plotted against published sets of genes that have previously been shown to define a specific lineage committed state. TBX3-induced ESCs were particularly enriched for mesoderm and endoderm class genes (Figures 3G and S2O) at the expense of trophectoderm class genes, whereas no specific regulation of ectoderm class genes was observed (Figure 3H). Also, principle component analysis and hierarchical clustering positioned the transcriptome of TBX3-induced samples within the three germ layers toward DE (Figures 3I and 3J). In summary, we show that TBX3 induces a subset of marker genes labeling mesoderm and endoderm and serves as a regulator of the mesendoderm transcriptional program.

(B) IF of E3.5 blastocyst for OCT4 (red) and TBX3 (green). Scale bars, 20 μm. Nuclei in DAPI (blue).
(C–E) TBX3 expression in postimplantation mouse embryos. (C) *Tbx3* mRNA in situ hybridization at E6.25 (prestreak) and E7.5 (midstreak). exVE, extraembryonic visceral endoderm. Arrows depict *Tbx3*-positive cells within the proximoposterior epiblast at E6.25 and mesoderm at E7.5. (D) *Tbx3* mRNA in whole mounts of wild-type embryos at E7.75 and E8.25. (E) Z-section of an E6.5 TBX3-GFP reporter embryo. Nuclei in DAPI (blue). Scale bars, 100 μm.
(F and G) *tbx3* expression in *Xenopus*. (F) Temporal expression of *tbx3* during early *Xenopus* embryogenesis. *tbx3* transcripts are maternally supplied. Zygotic expression starts at stage 10 and increases during gastrulation. *gapdh* as loading control. Negative control represents a −RT reaction with *gapdh*. (G) Spatial expression of *tbx3* at stages indicated during *Xenopus* development. *tbx3* is detected in the invaginating mesoderm during gastrulation. White arrowheads, *tbx3*-positive ectodermal cells; red arrowheads, *tbx3* expression in the developing cardiac region. m, mesoderm; cm, cardiac mesoderm. Scale bars, 0.5 mm.
See also Figure S5.

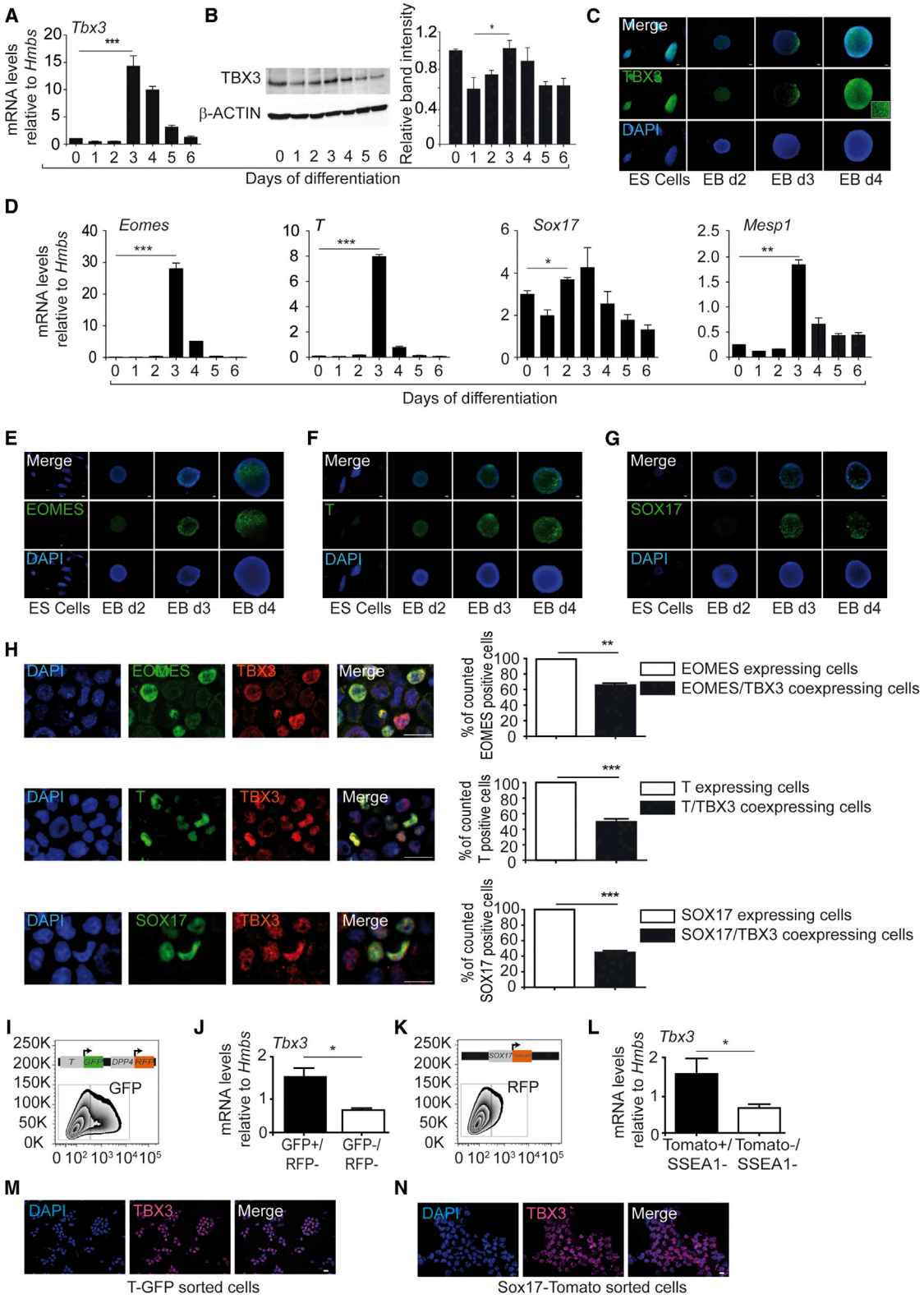

(legend on next page)

TBX3 Directs Cell Fate toward Mesendoderm-Derived Tissues

We also found TBX3 to be expressed in early cardiac progenitors during mouse and *Xenopus* development (Figures 1D and 1G). We therefore assessed whether late mesendoderm-derived tissues were likewise induced upon TBX3 overexpression in prolonged ESC differentiation cultures. At late time points of differentiation, EBs overexpressing TBX3 showed an increase in pancreatic differentiation indicated by *Hnf1β* and *Pdx1* RNA levels (Figure 4A). IF shows few scattered PDX1-positive cells under control conditions, whereas large clusters of pancreatic progenitors are detected in Dox-induced cultures (Figure 4B). Similarly, increased hepatic differentiation is shown by elevated *Hnf4α* and Albumin (*Alb*) RNA levels (Figures 4C and 4D). For mesoderm derivatives, TBX3 induction during the first 2 days of EB differentiation significantly enhanced the generation of beating cardiomyocytes (Movies S1 and S2; Figures 4E–4H), accompanied by increased mRNA levels of early cardiac-specific transcription factors *Mesp1* and *Nkx2.5* (see Figure 3D). Markers for the first and second heart field were induced to a similar extent (Figure 4E). Interestingly, cardiac induction was most efficient when TBX3 was induced early (days 0–2 and 0–4) during differentiation, whereas TBX3 induction following day 4 did not further promote cardiac differentiation. Atrial and ventricular markers were expressed at comparable levels (Figure 4F). We further confirmed cardiac induction by protein expression of α-ACTININ (Figure 4G) and assessment of beating clusters as well as beating intensity under the respective culture conditions (Figure 4H). Vascular markers (*CD31*, *VEGF-A*, *KDR*) were additionally increased, indicating that TBX3 acts early during the generation of the common cardiovascular progenitor (Figure 4I). Taken together, our data establish that expression of TBX3 early in differentiation promotes enhanced formation of definitive endoderm and mesoderm as well as respective later stage derivatives, namely pancreas, liver, and heart.

TBX3 Acts via a NODAL Signaling Dependent, Non-Cell-Autonomous Mechanism to Direct Mesendodermal Cell Fate

Secreted signaling molecules such as WNT3a, BMP4, and NODAL are required for lineage commitment during gastrulation onset (Zorn and Wells, 2009). Thus, we further investigated our microarray data to identify an impact of TBX3 on any of these three factors. Interestingly, mRNA expression of *Nodal* and its target genes were significantly increased in TBX3-overexpressing cells, whereas *Bmp4* was significantly downregulated (Figures 5A and 5B). Because NODAL signaling acts as one of the key pathways required for induction of mesendoderm both in vivo and in vitro (Arnold and Robertson, 2009), we investigated the relationship between TBX3 and NODAL signaling.

Nodal expression levels were significantly upregulated in TBX3-overexpressing cells via qPCR (Figure 5C). Moreover, phosphorylated SMAD2-levels, the major transducer of activated NODAL signaling, were significantly increased in TBX3-overexpressing cells (Figures 5E and 5F). We analyzed direct (responding to SMAD2/3 activation in the absence of protein synthesis) and indirect SMAD2/3 target genes (presence of protein synthesis) (Guzman-Ayala et al., 2009) and found both to be enriched in TBX3-overexpressing samples (Figures 5G and 5H). Blocking NODAL/SMAD2 signaling (ALK4/5/7 inhibitor) significantly attenuated the TBX3-inductive effects as shown by reduced expression of *Eomes*, *Nodal*, *Hex1*, and *FoxA2* (Figure 5I). To address binding of TBX3 on the *Nodal* promoter, we performed ChIP using TBX3-specific antibodies. We found a significant TBX3 enrichment on a highly conserved T-box binding element within the promoter region of the *Nodal* gene (Figure 5D; Figures S4A and S4B).

Due to the inductive impact of TBX3 on NODAL expression, we hypothesized that TBX3 affects cell specification via enhancing paracrine NODAL signaling (non-cell-autonomous mechanisms). We combined fluorophore-labeled iTBX3 cells (expressing the fluorophore tdTomato

Figure 2. TBX3 Expression in Differentiating ESCs

(A–C) TBX3 expression during EB-based ESC differentiation. (A) qPCR analysis; (B) immunoblot and quantification of three independent experiments; (C) whole-mount IF of TBX3 in differentiating EBs.

(D–G) Expression of lineage-specific markers (EOMES, T, SOX17, and MESP1) during ESC differentiation: (D) gene expression; (E–G) protein expression.

(H) IF shows coexpression of TBX3 with EOMES (upper panel row), T (middle panel row), and SOX17 (lower panel row) in differentiating ESCs (day 4). Quantifications of counted cells as bar graphs on the right.

(I) FACS of T-GFP/DPP4-RFP knockin ESCs on day 4 of differentiation; inset, description of reporter alleles.

(J) *Tbx3* gene expression in cell populations outlined in (I).

(K) FACS plot of SOX17-RFP knockin ESCs on day 4 of differentiation; inset shows description of reporter alleles.

(L) *Tbx3* expression in cell populations outlined in (K); pluripotent cells were depleted by SSEA1 staining.

(M) TBX3 immunostaining (magenta) of FACS sorted T-GFP-positive and DPP4-RFP-negative cells.

(N) TBX3 immunostaining (magenta) of SOX17-RFP-positive and SSEA1-negative cells. Scale bars, 20 μm. Nuclei in DAPI (blue). Error bars = SEM. n = 3 for all experiments in biological replicates.

*p < 0.05; **p < 0.01; ***p < 0.001. See also Figure S1.

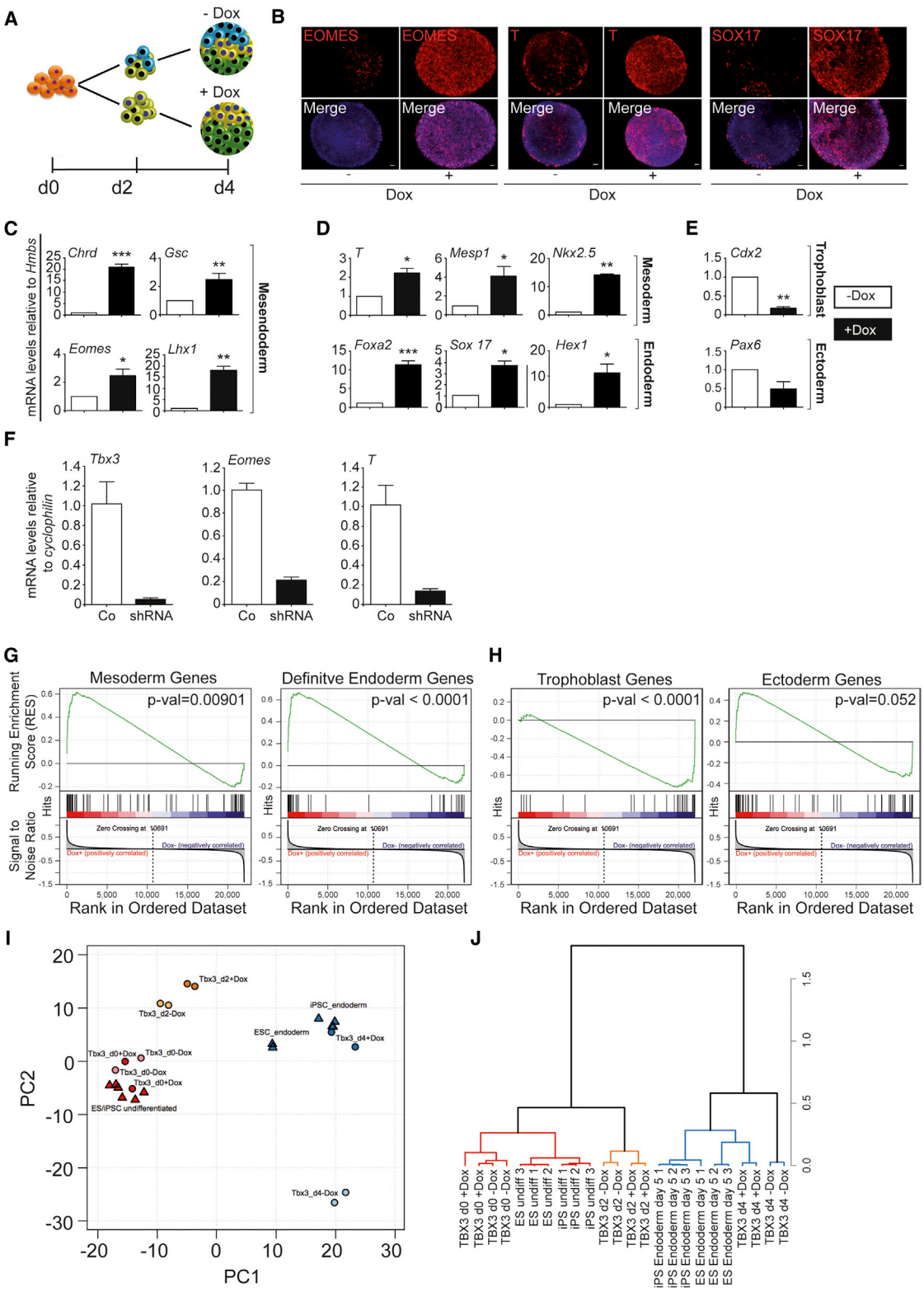

(legend on next page)

after lentiviral transduction) and unlabeled control cells in a chimeric EB culture system. Both cell lines were mixed at the indicated ratios, and TBX3 expression was induced by Dox. Nontreated cells served as controls (Figure S3A). Labeled and unlabeled cells were subsequently separated by FACS, and marker genes were quantified. We found significantly increased expression of early mesendoderm markers, such as *Lhx1* and *Eomes* (Figure S3B) in TBX3-overexpressing cells but interestingly also in cells not overexpressing TBX3. Notably, these effects increase with rising numbers of TBX3-overexpressing cells in the mixed EBs. Similar effects were observed when conditioned medium (CM) from iTBX3 cells was applied to wild-type EBs (Figure 6A), showing a marked increase in the mRNA levels of *Eomes*, *T*, *FoxA2*, and *Mesp1* (Figure 6B) and increased protein levels of EOMES, T, and SOX17 (Figures 6C–6E). Of note, non-CM-treated wild-type cells behaved similar to –Dox CM (Figures 6C–6E). In line, the non-cell-autonomous effect of iTBX3-CM was also observed for late mesendoderm derivatives such as cardiac cells or pancreatic progenitors (Figures S3C–S3E).

NODAL regulates its own expression but also induces negative feedback loops in which e.g., LEFTIES inhibit NODAL activity (Arnold and Robertson, 2009). To verify this physiological loop in CM experiments (Figure 6A), we identified specific upregulation of *Nodal* itself, as well as *Lefty1* and *Lefty2* in samples treated with CM generated from TBX3-overexpressing cells (Figure 6F). This strongly points to increased levels of secreted NODAL protein upon TBX3 expression. To elucidate the requirement of secreted NODAL within our model, we used a NODAL antibody to block secreted NODAL protein in iTBX3 cultures. We observed a substantial reduction in the TBX3-mediated expression of several mesendodermal genes including *Eomes*, *T*, *Sox17*, and *FoxA2* as well as *Nodal* itself (Figure 6G; Figure S3F). Overall, these experiments provide evidence that the lineage promoting effects of TBX3 can be attributed in part to paracrine effects, whereby TBX3 alters expression of key developmental factors, in particular, secreted NODAL protein.

TBX3 Directly Regulates Key Mesendoderm Determinants

Provided TBX3 actions could be only partially explained via paracrine signaling mechanisms, we decided to further investigate cell-autonomous effects of TBX3 in mediating cell lineage specification. We measured direct transcriptional activity of TBX3 on the regulation of key factors for mesendoderm (EOMES), mesoderm (T), and DE (SOX17) development. Overexpression of TBX3 led to the activation of EOMES, T, and SOX17 reporter constructs (Figure 7A). To confirm a direct binding of TBX3 to the corresponding promoters in differentiating ESCs, we performed ChIP using TBX3-specific antibodies. We found significant TBX3 enrichment on highly conserved T-box binding elements (Figure S4A), specifically within the promoter regions of *Eomes*, *T*, and *Sox17* (Figures 7B–7D; Figures S4C–S4E) with no enrichment for *Fgf2* (Figure 7E). Thus, our data suggest that TBX3 can directly or indirectly activate a mesendodermal lineage specification program via transcriptional regulation of specific mesoderm and endoderm transcription factors, and partly through activation of a NODAL/SMAD2 signaling cascade.

OCT4 has been shown to bias differentiation toward mesendoderm in ESCs and is known to activate the TBX3 promoter (Thomson et al., 2011). We asked whether TBX3 also regulates OCT4 levels during ESC differentiation. Indeed, OCT4 mRNA and protein expression levels were significantly elevated at day 2 and day 4 of differentiation following TBX3 induction (Figures 7F and 7G). Regulation of OCT4 by TBX3 was further corroborated using reporter assays, whereby TBX3 overexpression significantly enhanced OCT4 reporter activity (Figure 7H). The direct occupancy of TBX3 on the OCT4 promoter and vice versa has been shown previously (Figure S1; Thomson et al., 2011).

Figure 3. TBX3 Promotes Mesoderm and Endoderm

(A) Illustration of the differentiation protocol. EBs were generated over time from pluripotent ESCs at day 0 (orange) and markers from all three germ layers (ectoderm, blue; mesoderm, yellow; endoderm, green) were generated in –Dox samples, whereas mesoderm and endoderm were upregulated in the +Dox condition.

(B) Whole-mount IF in iTBX3 EBs (day 4) for Eomes (left panel), T (middle panel), and Sox17 (right panel) (all in red) upon TBX3 induction (±Dox). All scale bars are 20 μm. Nuclei in DAPI (blue).

(C–E) qPCR analysis showing expression of marker genes at day 4 of differentiation: (C) mesendoderm, (D) mesoderm and endoderm, (E) trophoblast and ectoderm upon TBX3 induction via doxycycline (±Dox). n = 3 for all experiments in biological replicates.

(F) TBX3 shRNA shows reduced levels of *Tbx3*, *T*, and *Eomes* expression levels already at EB day 1 after a 4 day feeder-free ESC condition. n = 2 for all experiments in biological replicates.

(G and H) Genome-wide transcriptional profiling followed by gene set enrichment analysis highlights that TBX3 selectively enriches mesoderm and endoderm (G) at the expense of trophoblast genes (H).

(I) Principal component analysis (PCA) positions TBX3-induced cells (TBX3_d4+dox) close to endoderm.

(J) Hierarchical clustering of TBX3-expressing EBs overlaps with published transcriptomes from DE (Christodoulou et al., 2011).

*p < 0.05; **p < 0.01; ***p < 0.001. See also Figure S2.

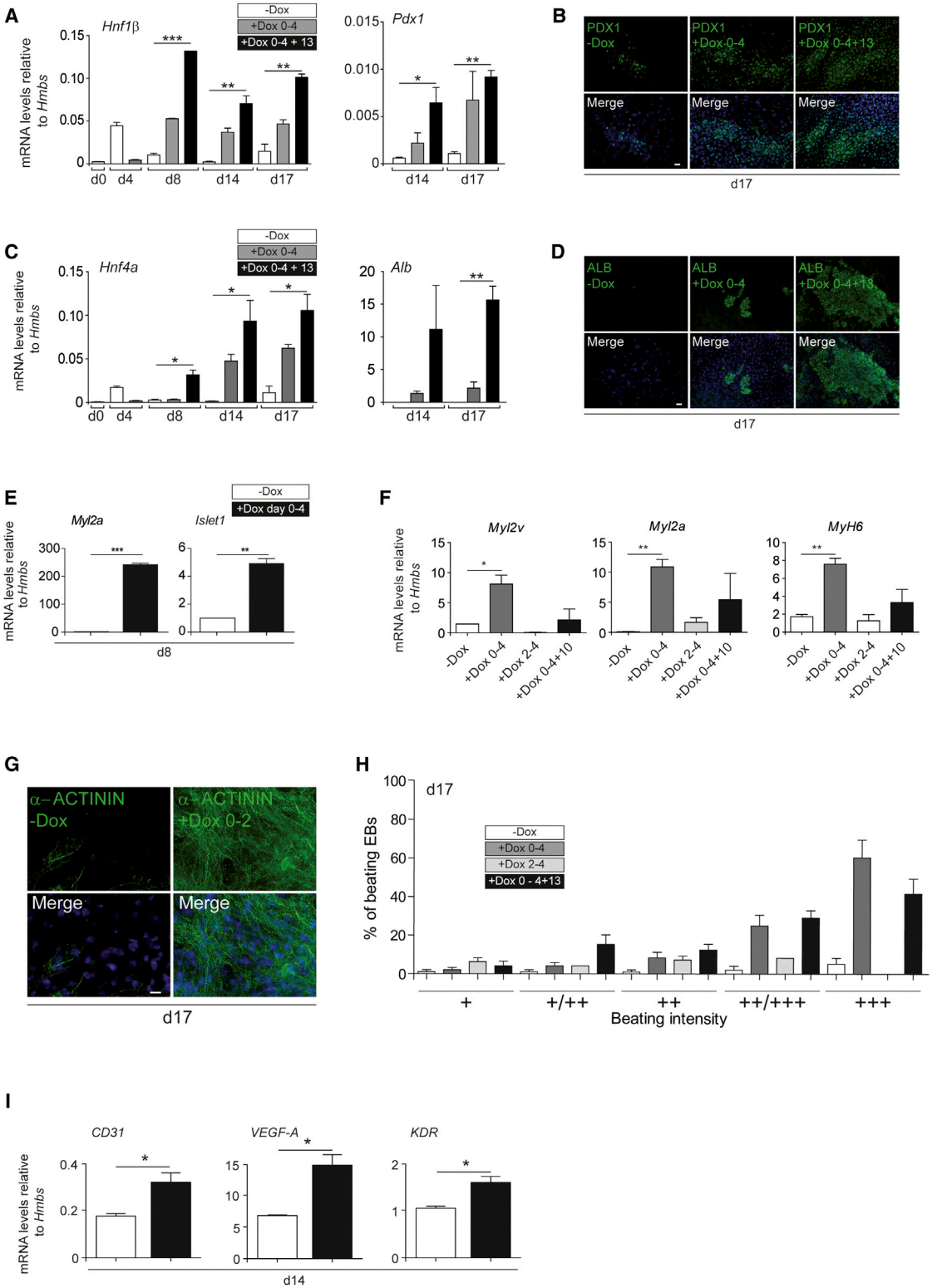

(legend on next page)

Finally, we overexpressed OCT4 alone or in combination with TBX3 and investigated effects on promoter activity of EOMES and SOX17 luciferase reporter constructs. In line with previous reports (Stefanovic et al., 2009), elevated OCT4 levels in ESCs enhanced the promoter activity of *Eomes* and *Sox17*. Coexpression of TBX3 and OCT4 significantly increased the luciferase activity of both promoters (Figure 7I).

TBX3 Is Entwined in Complex Regulatory Mechanisms with Closely Related T-Box Family Members during Early Development

Next, we aimed to investigate the role of TBX3 in *Xenopus laevis* as a vertebrate in vivo system performing morpholino-oligonucleotide (MO)-mediated loss-of-function experiments (Figures S5A and S5B). Cardiac development in *Xenopus* has recently been shown to follow a similar mechanism than in higher vertebrates (Gessert and Kühl, 2009). Targeted injection of *tbx3* MO into the presumptive heart region of *Xenopus* embryos resulted in cardiac malformations, edema formation, and a reduced heart beating. Thus, TBX3 loss of function in the *Xenopus* heart faithfully recapitulates the mouse phenotype (Figures S5C–S5E).

To test the requirement of TBX3 during early lineage commitment of mesendoderm derivatives, we injected *tbx3* MO into the marginal region of the two dorsal blastomeres at the 4-cell stage. Subsequent marker gene analysis at stage 10 and 10.5 revealed downregulation of *t* and *gsc* expression, respectively (Figures S7A and S7B). This indicates requirements of TBX3 for proper mesendodermal development in *Xenopus* embryos, thereby further substantiating our in vitro findings in ESCs.

Given the central role of TBX3 in mesendoderm lineage specification in vitro, we had anticipated a more global response to the loss of TBX3 in vivo, with greater changes in the expression of mesendodermal genes. We also could not detect an obvious gastrulation phenotype upon gross inspection of embryos. Furthermore, the lack of an early gastrulation phenotype in TBX3-deficient mice (Davenport et al., 2003) prompted us to hypothesize a scenario where potential compensatory mechanisms may be present. To identify potential compensatory factors, we reanalyzed several T-box factors in terms of their evolutionary proximity (Figure S6A). The analog TBX2 has previously been implicated to show functional redundancy with TBX3 during atrioventricular canal formation (Singh et al., 2012). Accordingly, TBX3 shows the highest relationship with TBX2 and to a lesser degree with TBX5 or TBX4. From a developmental point of view, TBX6 shows the highest overlap with TBX3 in expression in vitro (Pereira et al., 2011) and in vivo (Hadjantonakis et al., 2008), albeit evolutionary relationship with TBX3 is not that pronounced (Figure S6A). Based on this, we chose TBX2 and TBX6 for further analysis. In line with our hypothesis, we initially analyzed the expression of TBX2 and TBX6 in response to TBX3 overexpression in iTBX3-ESCs. Upon TBX3 induction, expression levels of TBX2 were almost abolished as shown by mRNA and protein levels (Figure S7C). Similar reductions on protein levels, but not as pronounced on mRNA levels were detected for TBX6 (Figure S7C).

We finally performed loss-of-function analysis in *Xenopus* using different combinations of MOs specifically targeting *tbx2* (Cho et al., 2011), *tbx3*, and *tbx6* (Tazumi et al., 2008) and analyzed gastrulation in more detail. Loss of TBX3 or TBX2 individually resulted in a delay of gastrulation movements as indicated by a moderately opened blastopore at stage 13 when control MO-injected embryos already closed the blastopore (Figure S7D). During subsequent development, these moderately opened blastopores closed, explaining the lack of any gastrulation phenotype at later stages. Only in some cases, the phenotype was severe and affected embryos did not recover. However, upon coinjection of *tbx2* and *tbx3* MO almost all embryos revealed a gastrulation phenotype. Taken together, these data indicate the functional redundancy of TBX3 and TBX2. Interestingly, loss of TBX6 resulted neither in delayed gastrulation movements, nor in a further increase in the percentage of phenotype or the severity of the phenotype (data not shown), indicating the specificity of the effects observed upon loss of TBX2 or TBX3. In summary, these data indicate the requirement of T-box transcription factors for proper gastrulation movements and that some T-box factors, e.g., TBX2 and TBX3 act in a redundant fashion in this context.

In summary, TBX3 is not only required to maintain pluripotency, but also to promote lineage determination via cell-autonomous regulation of key lineage determining transcription factors, at least in part additive to OCT4. Moreover, TBX3 acts non-cell-autonomously via direct activation of NODAL signaling, which, in turn, impacts

Figure 4. TBX3 Expression Promotes Mature Mesendodermal Cell Types

(A–G and I) TBX3 contributes to both pancreatic, hepatic, and cardiovascular lineage specification as assessed by qPCR (A, C, E, F, and I) and IF (B, D, and G) at the indicated time points (*pancreatic*: *Hnf1β*, PDX1; *hepatic*: Hnf4α; ALB, albumin; *cardiac*: *Myl2a*, *Islet1*, *Myl2v*, *Myh6*, and α-ACTININ; *vascular*: *CD31*, *VEGF-A*, *KDR*). All scale bars are 20 μm. Nuclei in DAPI (blue).

(H) Assessment of cardiac beating cluster percentage (y axis) and intensity (x axis) upon different Dox-treatment regimens. Error bars indicate standard error of the means (SEM). n = 3 for all experiments in biological replicates.

*p < 0.05; **p <0.01; ***p < 0.001. See also Figures S4, S6, and S7 and Movies S1 and S2.

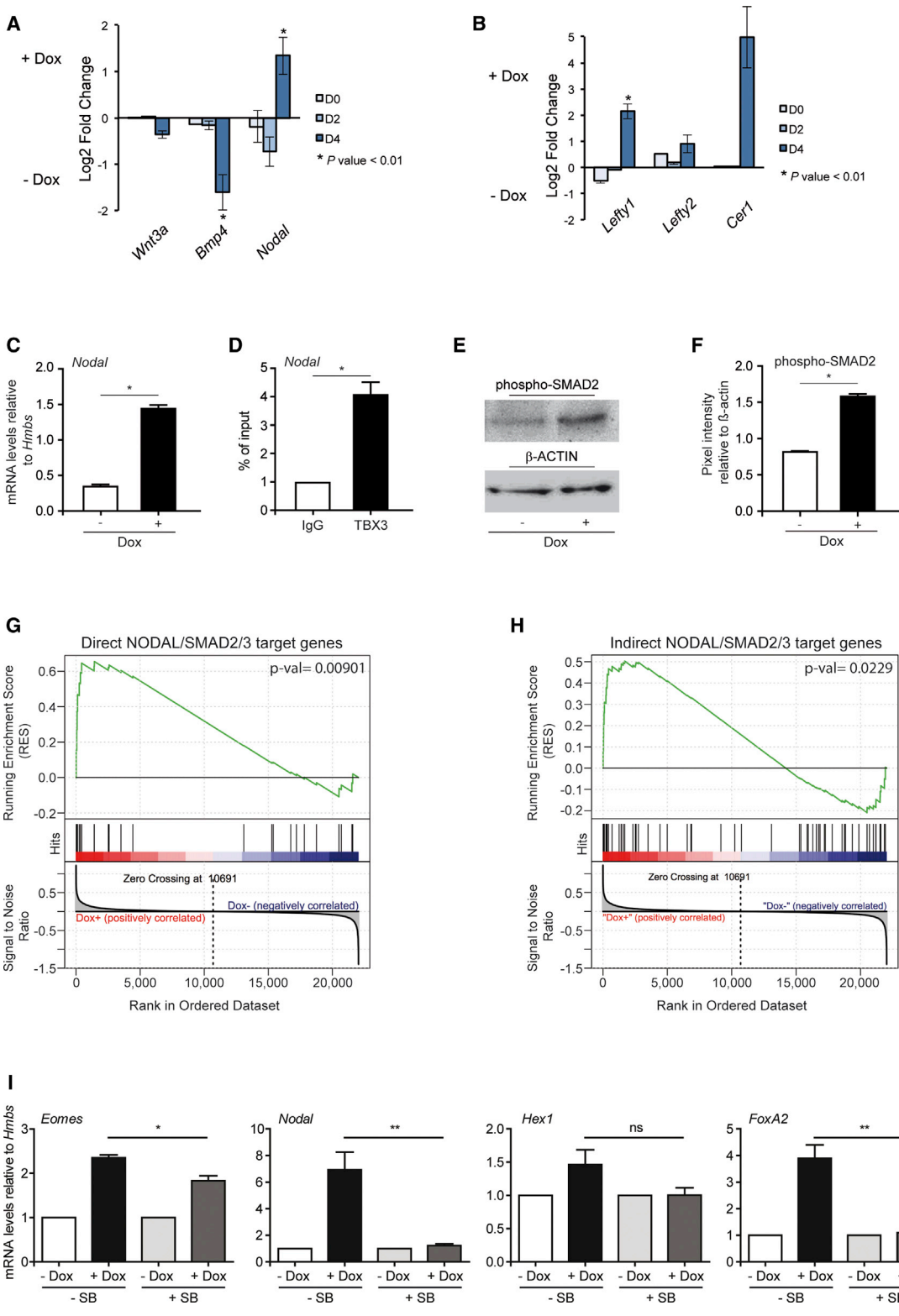

(legend on next page)

on the specification of DE and anterior mesoderm derivatives (Figure S6B).

DISCUSSION

TBX3 represents a unique member of the T-box family of transcription factors, due to its role in maintaining ground state pluripotency of murine ESCs. Recently, subsets of pluripotency-maintaining factors, namely, NANOG, OCT4, KLF5, and TBX3, have been shown to adopt new roles during lineage specification and have been globally defined as "mesendoderm class embryonic stem cell genes." However, detailed underlying insights how these transcription factors orchestrate cell-fate decisions, remain largely elusive. In the current study, we aimed to dissect the molecular function of TBX3 during early embryonic development.

The preimplantation expression pattern of TBX3 matches well with other mesendodermal pluripotency factors, such as OCT4 or KLF5 (Thomson et al., 2011), which together colocalize in the ICM of the late-stage blastocyst. Subsequently, TBX3 expression becomes rapidly restricted to the posterior proximal pole of the epiblast before a visible primitive streak has formed. Similarly, we found *tbx3* expression at the dorsal blastopore lip in *Xenopus*. TBX3 expression within the posterior side of the gastrulating embryo correlates well with the expression of NODAL, BRACHYURY, EOMES, and OCT4 (Morris et al., 2012). Midstreak embryos (E7.5) display robust expression of TBX3 in the proximal mesoderm. In ESCs, endogenous TBX3 expression coincides with crucial mesendoderm markers (EOMES, T, SOX17) and directly activates their promoters to drive mesendoderm. Further, TBX3 acts in concert with the histone demethylase JMJD3 to allow the activation of EOMES during DE formation (Kartikasari et al., 2013).

Already at the pluripotency state of ESCs TBX3 occupies promoters of "mesendodermal pluripotency genes" (*Oct4* and *Klf4* and *-5*) and of key lineage determining factors (*Sox9*, *Nkx6.1*, *Eomes*). It is therefore conceivable that TBX3 implements a functional switch during the exit from pluripotency toward embryonic lineage commitment. TBX3 facilitates cellular reprogramming via direct binding and activation of the OCT4 promoter (Han et al., 2010). Notably, it has been previously shown that OCT4 also binds the TBX3 promoter (Thomson et al., 2011). Therefore, it is particularly interesting that our data suggest inductive effects of both TBX3 and OCT4 in the transition from pluripotency to mesendoderm specification.

TBX3 is also expressed in the extraembryonic visceral endoderm (ExVE) and VE overlying the epiblast in pre- and midstreak embryos. In pregastrulation embryos, NODAL signaling pathways, both SMAD2-dependent and -independent, are crucially involved in defining the polarity of the pregastrulation embryo (Brennan et al., 2001). This requires interactions between the epiblast and the two extraembryonic tissues. The non-cell-autonomous TBX3 function to induce mesendoderm via enhanced NODAL secretion possibly involves the TBX3-expressing cells of the ExVE. We identify a central role for NODAL as an immediate target of TBX3 actions and demonstrate that blockade of the NODAL/SMAD2 pathway significantly detains TBX3-inductive effects. Moreover, extensive dispersion between the VE and DE leading to epiblast-derived organs containing extraembryonic elements is present (Kwon et al., 2008).

TBX3-null mice die around developmental stage E12.5 due to both cardiac and yolk sac defects. These mice exhibit a smaller sinoatrial node and die from AV blockage and ventricular bradycardia (Frank et al., 2012). Our data on TBX3 loss of function in the *Xenopus* heart faithfully recapitulate this phenotype. To our knowledge, a precise analysis of TBX3 mutant mouse embryos at early gastrulation stages has not yet been performed, which could potentially identify previously unrecognized spatiotemporal

Figure 5. TBX3 Activates a Nodal/Smad2 Signaling Cascade

(A and B) Genome-wide transcriptional profiling to identify fluctuations in developmental signaling pathways in response to overexpression of TBX3 (+Dox). (A) Significant upregulation of the *Nodal* gene within the Dox-treated sample, whereas *Wnt3a* and *Bmp4* are downregulated. (B) NODAL target genes *Lefty1*, *Lefty2*, and *Cer1* are upregulated in the +Dox-treated sample.

(C) qPCR analysis for *Nodal* mRNA in ±Dox cells at day 4 of differentiation. n = 3 in biological replicates.

(D) Quantification of DNA fragment enrichment by ChIP using TBX3-specific antibody relative to control isotype measured by qPCR utilizing region specific *Nodal* primers (Figures S4A and S4B).

(E and F) WB analysis for phosphorylated SMAD2 in day 4 EBs overexpressing TBX3 (+Dox) and control EBs (–Dox). TBX3-induced EBs contain higher levels of phosphorylated SMAD2 (F). n = 3 for biological replicates; quantification of three independent experiments is from (E).

(G and H) TBX3 activates direct (G) and indirect (H) target genes of the NODAL/SMAD2 pathway. (G) A set of published genes showing direct (in absence of protein synthesis) or (H) indirect (in presence of protein synthesis) regulation upon SMAD2 phosphorylation was used for gene set enrichment analysis of ±Dox samples. Error bars = SEMs.

(I) qPCR analysis for *Eomes*, *Nodal*, *Hex*, and *FoxA2* mRNA levels in ±Dox cells at day 4 of differentiation with/without ALK4/5/7 inhibitor SB431542 (10 μM). n = 2 for independent experiments, each in biological triplicates.

*p < 0.05; **p < 0.01; ***p < 0.001. See also Figures S3 and S4.

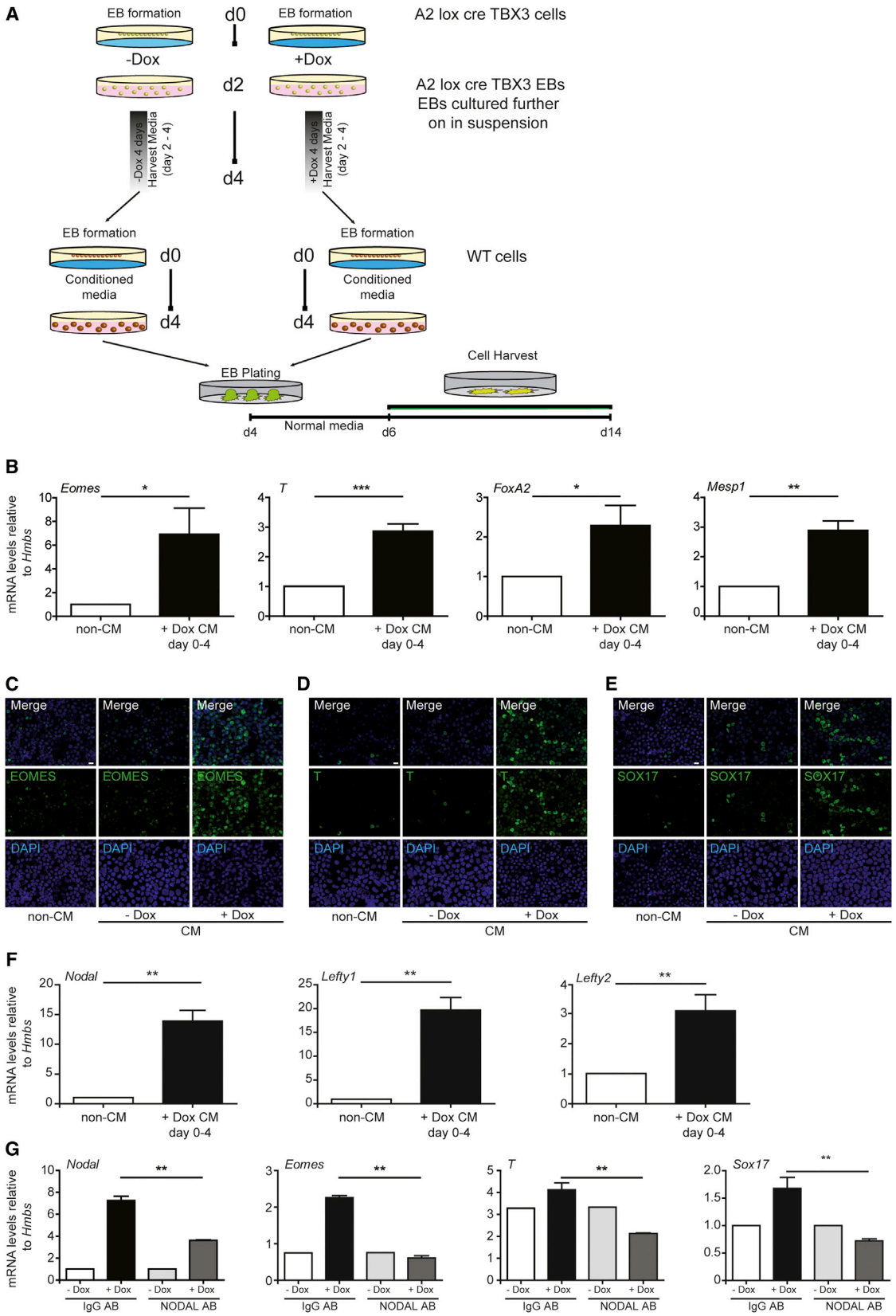

(legend on next page)

abnormalities of primitive streak formation. In fact, monogenetic knockouts of certain genes result in moderate or no gastrulation defects, whereas combined ablation strategies result in more severe gastrulation defects (Solloway and Robertson, 1999; Song et al., 1999).

We found that loss of either TBX2 or TBX3 but not TBX6 results in a delay of gastrulation in *Xenopus*. We therefore propose that T-box factors act in a redundant but also specific manner to allow ongoing gastrulation. Notably, T-box genes are known to operate in a complex network to regulate region- and species-specific gene expression and developmental fate (Goering et al., 2003). Accordingly, T-box factors have now been classified into three subtypes, namely, additive, competitive, and combinatorial (Goering et al., 2003). They show overlapping expression patterns in numerous tissues, while exhibiting distinct spatiotemporal expression and functions in other compartments. This has several implications for dissecting the individual contribution of a single T-box gene within specific processes and highlights that any genetic manipulation of T-box genes such as gain- or loss-of-function analysis must be carefully taken to be context dependent.

Specifically, functional redundancy between the paralogous TBX2 and TBX3 has previously been identified during atrioventricular canal, mammalian secondary palate formation (Singh et al., 2012) as well as during *Xenopus* eye development (Takabatake et al., 2002). In this respect, TBX2/TBX3 double-knockout mice display greater overall embryonic growth defects (lethal as early as E9.5) compared to single-knockout mice (lethal at E12.5) (Mesbah et al., 2012). Tbx6 knockout mice exhibit reduced NODAL levels in early development stages (Carreira et al., 1998). This molecular abnormality would appear to somewhat overlap with TBX3 functions. However, during *Xenopus* gastrulation we could not detect any functional redundancy between TBX3 and TBX6.

Altogether, our results describe facets of TBX3 actions within early cell-fate determination. We demonstrate that TBX3 is dynamically expressed during specification of the mesendoderm lineages in differentiating ESCs in vitro and at specific sites during gastrulation onset in developing mouse and *Xenopus* embryos. We depict that TBX3 exerts dual cell-autonomous and non-cell-autonomous effects by directly activating core mesendoderm lineage specification factors and influencing NODAL/SMAD2 signaling, respectively. Moreover, we show that TBX3 acts together with OCT4 to promote mesendoderm specification. Finally, we display a functional redundancy between TBX3 and the closely related family member TBX2, pointing to a complex compensatory mechanisms. We propose a model in which TBX3 orchestrates a complex network of downstream effects within the T-box family members to direct pluripotent cells toward a mesendodermal fate. A more comprehensive understanding of the role of pluripotency factors in subsequent lineage commitment may provide important insights about tightly regulated developmental processes such as gastrulation.

EXPERIMENTAL PROCEDURES

Full methods accompany this paper in the Supplemental Experimental Procedures.

Generation of iTBX3 ESCs

One day before the nucleofection procedure, A2lox.cre cells were exposed to 1 μg/ml of doxycycline to induce Cre recombinase. ESCs were nucleofected using the Nucleofector Technology (Lonza) according to the manufacturer's procedures. The Nucleofector Kit for Mouse Embryonic Stem Cells was used according to manufacturer's instructions and 10 μg of DNA (TBX3-p2lox vector) per 5 million parental A2lox.cre ESCs. Nucleofected cells were plated on neomycin-resistant, Mitomycin-C (Sigma) inactivated MEFs and selected 2 days after nucleofection with neomycin (400 μg/ml).

Gene Expression Microarray Analysis

The Agilent DNA microarray data were preprocessed and normalized by the limma package (Smyth, 2004). The Affymetrix DNA microarray data (GSE27087) were normalized by RMA algorithm implemented in Affymetrix power tools. The investigated gene sets were collected from Mouse Genome Informatics database (Finger et al., 2011) and literature.

Figure 6. TBX3 Acts via Non-Cell-Autonomous Mechanisms to Direct Cell Fate

(A) Illustration of the treatment strategy to generate conditioned medium (CM) from iTBX3 cells and subsequent generation of EBs.

(B) qPCR for *Eomes*, *T*, *Foxa2*, and *Mesp1* in differentiating wild-type ESCs cultured in either non-CM or +Dox-CM days 0–4 from iTBX3 cells on day 4.

(C–E) IF of differentiating wild-type ESCs cultured in either non-CM or CM from iTBX3 cells (either ±Dox) on day 4; wild-type cells treated with +Dox-CM days 0–4 of iTBX3 cells show a higher protein expression of the depicted markers (C) EOMES, (D) T, and (E) SOX17. All scale bars are 20 μm. Nuclei in DAPI (blue). n = 3 in biological replicates.

(F) qPCR analysis for *Nodal*, *Lefty1*, and *Lefty2* mRNA levels in either non-CM or +Dox-CM days 0–4 from iTBX3 cells on day 4.

(G) *Nodal*, *Eomes*, *T*, and *Sox17* mRNA levels in untreated (-Dox) and Dox-treated (+Dox) iTBX3 cells at day 4 of differentiation in ± 3 μM NODAL-blocking antibody, (n = 2) independent experiments, each in biological triplicates.

*p < 0.05; **p < 0.01; ***p < 0.001. See also Figure S3.

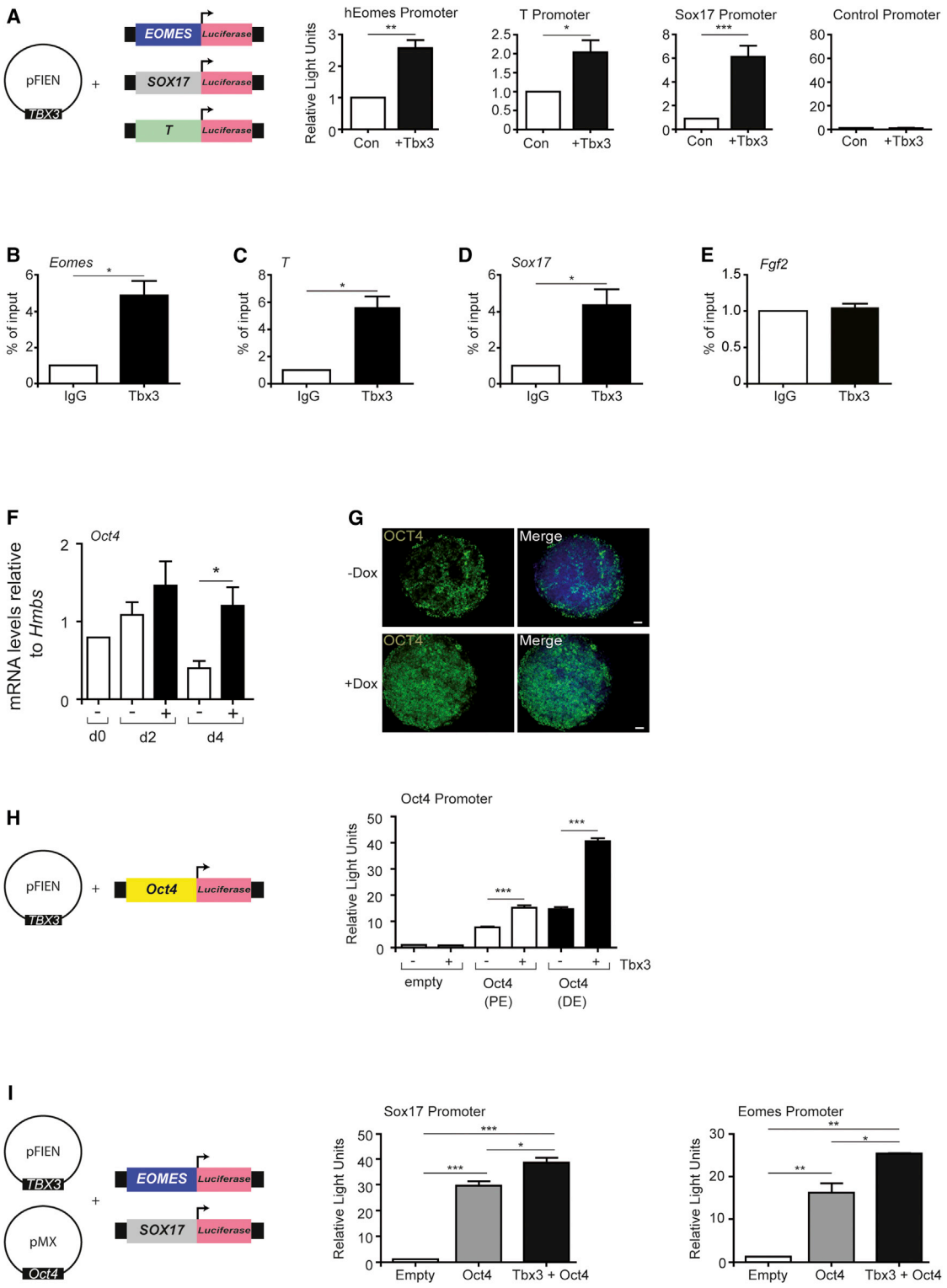

Figure 7. TBX3 Directly Regulates Key Factors for Mesendoderm Induction

(A) Luciferase reporter of EOMES (left bar), T (middle bar), and SOX17 (right bar) promoters were cotransfected in HEK cells with a TBX3-expression plasmid and assessed for luciferase activity, (n = 3) biological replicates. Similar data with iTBX3 ESCs (data not shown). (B–E) qPCR quantification of DNA fragments enrichment by ChIP using TBX3-specific antibody relative to control isotype for (B) *Eomes*, (C) *T*, (D) *Sox17*, and (E) *Fgf2*. n = 3 for biological replicates.

(legend continued on next page)

Quantitative One-Step Real-Time RT-PCR

Quantitative one-step real-time RT-PCR analysis was implemented as previously described (Kleger et al., 2007, 2010; Liebau et al., 2007).

Chromatin Immunoprecipitation

Approximately, 2×10^6 differentiated ESCs were crosslinked by adding formaldehyde directly to the medium to a final concentration of 1% (w/v) at room temperature. The ChIP Assay kit (ChIP-IT Express Enzymatic, Active Motif, #53009) was used according to the manufacturer's instructions. Details are in the Supplemental Information.

Statistical Analysis

If not stated otherwise, SEMs are indicated by error bars. For comparisons of two groups, levels of significance were calculated with the unpaired Student's t test if not indicated otherwise. *$p < 0.05$; **$p < 0.01$; ***$p < 0.001$. Significances were calculated with Prism5 (GraphPad).

SUPPLEMENTAL INFORMATION

Supplemental Information includes Supplemental Experimental Procedures, seven figures, and two movies and can be found with this article online at http://dx.doi.org/10.1016/j.stemcr.2013.08.002.

ACKNOWLEDGMENTS

The authors thank R. Köhntop, S. Fischer, and S. Seltenheim for excellent technical assistance. This study was funded by the Deutsche Forschungsgemeinschaft (DFG, KL 2544/1-1, SL BO1718/4-1, MZ Ze432/5-2), German Foundation for Heart Research (F/34/11; to A.K. and S.L.), Boehringer-Ingelheim BIU (N5 to S.L.; C1 to A.K.), Helmholtz Gesellschaft (VH-VI-510 to T.M.B. and S.L.), Else-Kröner-Fresenius-Stiftung (2011_A200; to A.K. and S.L.), BMBF (MND-Net to S.L. and T.M.B., Systar to A.K.) A.K. is indebted to the Baden-Württemberg Stiftung for the financial support of this research project by the Eliteprogramme for Postdocs.

Received: June 18, 2013
Revised: August 6, 2013
Accepted: August 7, 2013
Published: August 29, 2013

REFERENCES

Arnold, S.J., and Robertson, E.J. (2009). Making a commitment: cell lineage allocation and axis patterning in the early mouse embryo. Nat. Rev. Mol. Cell Biol. *10*, 91–103.

Bamshad, M., Lin, R.C., Law, D.J., Watkins, W.C., Krakowiak, P.A., Moore, M.E., Franceschini, P., Lala, R., Holmes, L.B., Gebuhr, T.C., et al. (1997). Mutations in human TBX3 alter limb, apocrine and genital development in ulnar-mammary syndrome. Nat. Genet. *16*, 311–315.

Blair, K., Wray, J., and Smith, A. (2011). The liberation of embryonic stem cells. PLoS Genet. *7*, e1002019.

Brennan, J., Lu, C.C., Norris, D.P., Rodriguez, T.A., Beddington, R.S., and Robertson, E.J. (2001). Nodal signalling in the epiblast patterns the early mouse embryo. Nature *411*, 965–969.

Carreira, S., Dexter, T.J., Yavuzer, U., Easty, D.J., and Goding, C.R. (1998). Brachyury-related transcription factor Tbx2 and repression of the melanocyte-specific TRP-1 promoter. Mol. Cell. Biol. *18*, 5099–5108.

Chapman, D.L., Garvey, N., Hancock, S., Alexiou, M., Agulnik, S.I., Gibson-Brown, J.J., Cebra-Thomas, J., Bollag, R.J., Silver, L.M., and Papaioannou, V.E. (1996). Expression of the T-box family genes, Tbx1-Tbx5, during early mouse development. Dev. Dyn. *206*, 379–390.

Cheng, X., Ying, L., Lu, L., Galvão, A.M., Mills, J.A., Lin, H.C., Kotton, D.N., Shen, S.S., Nostro, M.C., Choi, J.K., et al. (2012). Self-renewing endodermal progenitor lines generated from human pluripotent stem cells. Cell Stem Cell *10*, 371–384.

Cho, G.S., Choi, S.C., Park, E.C., and Han, J.K. (2011). Role of Tbx2 in defining the territory of the pronephric nephron. Development *138*, 465–474.

Christodoulou, C., Longmire, T.A., Shen, S.S., Bourdon, A., Sommer, C.A., Gadue, P., Spira, A., Gouon-Evans, V., Murphy, G.J., Mostoslavsky, G., and Kotton, D.N. (2011). Mouse ES and iPS cells can form similar definitive endoderm despite differences in imprinted genes. J. Clin. Invest. *121*, 2313–2325.

Davenport, T.G., Jerome-Majewska, L.A., and Papaioannou, V.E. (2003). Mammary gland, limb and yolk sac defects in mice lacking Tbx3, the gene mutated in human ulnar mammary syndrome. Development *130*, 2263–2273.

Finger, J.H., Smith, C.M., Hayamizu, T.F., McCright, I.J., Eppig, J.T., Kadin, J.A., Richardson, J.E., and Ringwald, M. (2011). The mouse

(F and G) TBX3 induces OCT4 expression: (F) mRNA level of *Oct4* upon TBX3 induction (±Dox) at indicated time points. (G) Protein level of OCT4 whole-mount stained EBs upon TBX3 induction (±Dox) at day 4. All scale bars 20 μm. Nuclei in DAPI (blue). n = 3 for biological replicates.
(H) Schematic outline of OCT4 reporter assays (left panel). Luciferase reporter constructs with either proximal or distal OCT4 enhancer elements cotransfected into HEK cells together with a TBX3-expression plasmid and assessed for luciferase activity. n = 3 for biological replicates. Similar observations were made when iTbx3 ESCs were used (data not shown).
(I) HEK cells were cotransfected with the respective luciferase reporter constructs in the presence or absence of OCT4- and TBX3-expression plasmids (schematic outline, left panel) and assayed for promoter activity of Sox17 (middle panel) and Eomes (right panel). Similar observations were made when iTbx3 ESCs were used (data not shown). n = 3 for biological replicates.
*$p < 0.05$; **$p < 0.01$; ***$p < 0.001$. See also Figures S4 and S7.

Gene Expression Database (GXD): 2011 update. Nucleic Acids Res. *39*(Database issue), D835–D841.

Frank, D.U., Carter, K.L., Thomas, K.R., Burr, R.M., Bakker, M.L., Coetzee, W.A., Tristani-Firouzi, M., Bamshad, M.J., Christoffels, V.M., and Moon, A.M. (2012). Lethal arrhythmias in Tbx3-deficient mice reveal extreme dosage sensitivity of cardiac conduction system function and homeostasis. Proc. Natl. Acad. Sci. USA *109*, E154–E163.

Gessert, S., and Kühl, M. (2009). Comparative gene expression analysis and fate mapping studies suggest an early segregation of cardiogenic lineages in Xenopus laevis. Dev. Biol. *334*, 395–408.

Goering, L.M., Hoshijima, K., Hug, B., Bisgrove, B., Kispert, A., and Grunwald, D.J. (2003). An interacting network of T-box genes directs gene expression and fate in the zebrafish mesoderm. Proc. Natl. Acad. Sci. USA *100*, 9410–9415.

Guo, G., Huss, M., Tong, G.Q., Wang, C., Li Sun, L., Clarke, N.D., and Robson, P. (2010). Resolution of cell fate decisions revealed by single-cell gene expression analysis from zygote to blastocyst. Dev. Cell *18*, 675–685.

Guzman-Ayala, M., Lee, K.L., Mavrakis, K.J., Goggolidou, P., Norris, D.P., and Episkopou, V. (2009). Graded Smad2/3 activation is converted directly into levels of target gene expression in embryonic stem cells. PLoS ONE *4*, e4268.

Hadjantonakis, A.K., Pisano, E., and Papaioannou, V.E. (2008). Tbx6 regulates left/right patterning in mouse embryos through effects on nodal cilia and perinodal signaling. PLoS ONE *3*, e2511.

Han, J., Yuan, P., Yang, H., Zhang, J., Soh, B.S., Li, P., Lim, S.L., Cao, S., Tay, J., Orlov, Y.L., et al. (2010). Tbx3 improves the germ-line competency of induced pluripotent stem cells. Nature *463*, 1096–1100.

Hoogaars, W.M., Engel, A., Brons, J.F., Verkerk, A.O., de Lange, F.J., Wong, L.Y., Bakker, M.L., Clout, D.E., Wakker, V., Barnett, P., et al. (2007). Tbx3 controls the sinoatrial node gene program and imposes pacemaker function on the atria. Genes Dev. *21*, 1098–1112.

Horsthuis, T., Buermans, H.P., Brons, J.F., Verkerk, A.O., Bakker, M.L., Wakker, V., Clout, D.E., Moorman, A.F., 't Hoen, P.A., and Christoffels, V.M. (2009). Gene expression profiling of the forming atrioventricular node using a novel tbx3-based node-specific transgenic reporter. Circ. Res. *105*, 61–69.

Iacovino, M., Bosnakovski, D., Fey, H., Rux, D., Bajwa, G., Mahen, E., Mitanoska, A., Xu, Z., and Kyba, M. (2011). Inducible cassette exchange: a rapid and efficient system enabling conditional gene expression in embryonic stem and primary cells. Stem Cells *29*, 1580–1588.

Kartikasari, A.E., Zhou, J.X., Kanji, M.S., Chan, D.N., Sinha, A., Grapin-Botton, A., Magnuson, M.A., Lowry, W.E., and Bhushan, A. (2013). The histone demethylase Jmjd3 sequentially associates with the transcription factors Tbx3 and Eomes to drive endoderm differentiation. EMBO J. *32*, 1393–1408.

Kleger, A., Busch, T., Liebau, S., Prelle, K., Paschke, S., Beil, M., Rolletschek, A., Wobus, A., Wolf, E., Adler, G., and Seufferlein, T. (2007). The bioactive lipid sphingosylphosphorylcholine induces differentiation of mouse embryonic stem cells and human promyelocytic leukaemia cells. Cell. Signal. *19*, 367–377.

Kleger, A., Seufferlein, T., Malan, D., Tischendorf, M., Storch, A., Wolheim, A., Latz, S., Protze, S., Porzner, M., Proepper, C., et al. (2010). Modulation of calcium-activated potassium channels induces cardiogenesis of pluripotent stem cells and enrichment of pacemaker-like cells. Circulation *122*, 1823–1836.

Kwon, G.S., Viotti, M., and Hadjantonakis, A.K. (2008). The endoderm of the mouse embryo arises by dynamic widespread intercalation of embryonic and extraembryonic lineages. Dev. Cell *15*, 509–520.

Liebau, S., Vaida, B., Proepper, C., Grissmer, S., Storch, A., Boeckers, T.M., Dietl, P., and Wittekindt, O.H. (2007). Formation of cellular projections in neural progenitor cells depends on SK3 channel activity. J. Neurochem. *101*, 1338–1350.

Lu, R., Yang, A., and Jin, Y. (2011). Dual functions of T-box 3 (Tbx3) in the control of self-renewal and extraembryonic endoderm differentiation in mouse embryonic stem cells. J. Biol. Chem. *286*, 8425–8436.

Mesbah, K., Rana, M.S., Francou, A., van Duijvenboden, K., Papaioannou, V.E., Moorman, A.F., Kelly, R.G., and Christoffels, V.M. (2012). Identification of a Tbx1/Tbx2/Tbx3 genetic pathway governing pharyngeal and arterial pole morphogenesis. Hum. Mol. Genet. *21*, 1217–1229.

Morris, S.A., Grewal, S., Barrios, F., Patankar, S.N., Strauss, B., Buttery, L., Alexander, M., Shakesheff, K.M., and Zernicka-Goetz, M. (2012). Dynamics of anterior-posterior axis formation in the developing mouse embryo. Nat Commun *3*, 673.

Niwa, H., Ogawa, K., Shimosato, D., and Adachi, K. (2009). A parallel circuit of LIF signalling pathways maintains pluripotency of mouse ES cells. Nature *460*, 118–122.

Pereira, L.A., Wong, M.S., Lim, S.M., Sides, A., Stanley, E.G., and Elefanty, A.G. (2011). Brachyury and related Tbx proteins interact with the Mixl1 homeodomain protein and negatively regulate Mixl1 transcriptional activity. PLoS ONE *6*, e28394.

Price, F.D., Yin, H., Jones, A., van Ijcken, W., Grosveld, F., and Rudnicki, M.A. (2012). Canonical Wnt signaling induces a primitive endoderm metastable state in mouse embryonic stem cells. Stem Cells *31*, 752–764.

Singh, R., Hoogaars, W.M., Barnett, P., Grieskamp, T., Rana, M.S., Buermans, H., Farin, H.F., Petry, M., Heallen, T., Martin, J.F., et al. (2012). Tbx2 and Tbx3 induce atrioventricular myocardial development and endocardial cushion formation. Cell. Mol. Life Sci. *69*, 1377–1389.

Smyth, G.K. (2004). Linear models and empirical bayes methods for assessing differential expression in microarray experiments. Stat. Appl. Genet. Mol. Biol. *3*, Article3.

Solloway, M.J., and Robertson, E.J. (1999). Early embryonic lethality in Bmp5;Bmp7 double mutant mice suggests functional redundancy within the 60A subgroup. Development *126*, 1753–1768.

Song, J., Oh, S.P., Schrewe, H., Nomura, M., Lei, H., Okano, M., Gridley, T., and Li, E. (1999). The type II activin receptors are essential for egg cylinder growth, gastrulation, and rostral head development in mice. Dev. Biol. *213*, 157–169.

Stefanovic, S., Abboud, N., Désilets, S., Nury, D., Cowan, C., and Pucéat, M. (2009). Interplay of Oct4 with Sox2 and Sox17: a

molecular switch from stem cell pluripotency to specifying a cardiac fate. J. Cell Biol. *186*, 665–673.

Tada, S., Era, T., Furusawa, C., Sakurai, H., Nishikawa, S., Kinoshita, M., Nakao, K., Chiba, T., and Nishikawa, S. (2005). Characterization of mesendoderm: a diverging point of the definitive endoderm and mesoderm in embryonic stem cell differentiation culture. Development *132*, 4363–4374.

Takabatake, Y., Takabatake, T., Sasagawa, S., and Takeshima, K. (2002). Conserved expression control and shared activity between cognate T-box genes Tbx2 and Tbx3 in connection with Sonic hedgehog signaling during Xenopus eye development. Dev. Growth Differ. *44*, 257–271.

Tazumi, S., Yabe, S., Yokoyama, J., Aihara, Y., and Uchiyama, H. (2008). PMesogenin1 and 2 function directly downstream of Xtbx6 in Xenopus somitogenesis and myogenesis. Dev. Dyn. *237*, 3749–3761.

Thomson, M., Liu, S.J., Zou, L.N., Smith, Z., Meissner, A., and Ramanathan, S. (2011). Pluripotency factors in embryonic stem cells regulate differentiation into germ layers. Cell *145*, 875–889.

Ying, Q.L., Wray, J., Nichols, J., Batlle-Morera, L., Doble, B., Woodgett, J., Cohen, P., and Smith, A. (2008). The ground state of embryonic stem cell self-renewal. Nature *453*, 519–523.

Zorn, A.M., and Wells, J.M. (2009). Vertebrate endoderm development and organ formation. Annu. Rev. Cell Dev. Biol. *25*, 221–251.